J. Coat. Technol. Res., **5** (3) 327–334, 2008
DOI 10.1007/s11998-008-9084-x

The electrodeposition of polypyrrole on Al alloy from room temperature ionic liquids

Jun Nie, Dennis E. Tallman, Gordon P. Bierwagen

Abstract The direct electrodeposition of conjugated polymers onto active metals such as aluminum and its alloys is complicated by the concomitant oxidation of the metal that occurs at the positive potential required for polymer formation/deposition. We previously described an approach that uses electron transfer mediation to reduce the deposition potential of polypyrrole (PPy) on aluminum and aluminum alloy by nearly 500 mV, permitting film deposition from aqueous solution with nearly 100% current efficiency. In this report, 1-ethyl-3-methylimidazolium bis(trifluoromethanesulfonyl)imide ($EMIM^+TFSI^-$) has been successfully employed both as the growth medium and the supporting electrolyte for directly depositing uniform and conductive PPy coatings onto Al alloy 2024-T3 surface via a potentiodynamic technique. The depositions of PPy were carried out under cyclic voltammetric conditions from 0.3 M pyrrole in ionic liquid solutions. Film morphology was characterized by atomic force microscopy, optical microscopy, and scanning electron microscopy (SEM). Energy dispersive X-ray analysis and X-ray photoelectron spectroscopy verified that the $TFSI^-$ anion was incorporated into the polymer as the dopant ion. Thickness of the film was measured by SEM and film conductivity was determined by both a four-point probe technique and by conducting atomic force microscopy. Electrochemical activity of the film was assessed by cyclic voltammetry. Results from these preliminary studies will be reported.

Keywords Polypyrrole, Room temperature ionic liquids, Electrodeposition, Aluminum alloy

Presented at the 2007 FutureCoat! conference, sponsored by the Federation of Societies for Coatings Technology, in Toronto, Ont., Canada, on October 3–5, 2007.

J. Nie, D. E. Tallman (✉), G. P. Bierwagen
North Dakota State University, Fargo, ND, USA
e-mail: dennis.tallman@ndsu.edu

Introduction

Our research group has been exploring two types of active coatings for corrosion control of aluminum alloys, magnesium-rich coatings which function primarily by a cathodic protection mechanism,[1] and conjugated polymer (CP) coatings which also interact with the metal substrate by electrical and/or electrochemical interactions.[2–7] Such coatings are viewed to be less hazardous to human health and to the environment than currently used chromate-containing coatings. A limitation to the use of CPs as corrosion control coatings is the difficulty in casting such polymers as coatings, since CPs are insoluble in most solvents unless suitably derivatized. Thus, either functionalized polymers are used in these studies (i.e., the polymers are formed from monomers containing a side chain that imparts solubility and/or contain a dopant ion that imparts solubility) or the CP is incorporated as a pigment in a traditional polymeric binder.[5,8] We have recently discussed the various approaches to forming CP-based coatings and have detailed various aspects of their mechanism.[9]

Conjugated polymer films are readily formed by direct electropolymerization/deposition onto noble metals such as Pt and Au. However, the direct electrodeposition of CPs onto aluminum and its alloys is generally not feasible due to the positive potentials required for polymerization, potentials at which the metal oxidizes (corrodes), especially when carried out from aqueous solution. In the case of aluminum and its alloys, a high bandgap (i.e., electronically insulating) oxide forms under such conditions and an adherent, continuous CP film is difficult to achieve without resorting to special surface preparation strategies and electrolytes, and even then high monomer concentrations must be used and overoxidized polymer is often obtained.[10,11] Polymerization in the presence of surfactant anions, such as sodium dodecyl sulfate and

sodium dodecylbenzenesulfonate, have also been found to yield uniform CP films on the Al surface.[12–14]

Pyrrole (Py) has a large overpotential for oxidation at the alloy surface. This apparently results from the incompatibility of the rather hydrophobic Py monomer and the rather hydrophilic alloy (oxide) surface, an incompatibility that the surfactants noted above appear to minimize. An alternative approach developed in our laboratory uses electron transfer mediation (or catalysis) to reduce the deposition potential of polypyrrole (PPy) on aluminum and aluminum alloy by approximately 500 mV, permitting film deposition from aqueous solution with nearly 100% current efficiency.[15–17] The mediator used most often in this earlier work was the disodium salt of 4,5-dihydroxy-1,3-benzenedisulfonate (DHDBS, also known as Tiron®), which also served as the dopant or counter ion in the polymer, but other mediators appear promising and a mechanism has been proposed.[18] Galvanostatic electrodeposition of PPy in the presence of DHBDS leads to uniform, adherent, conducting, electroactive films.[15] Electrochemical atomic force microscopy studies[19] in combination with the potential-time curves obtained during galvanostatic electrodeposition of PPy[15] indicated that DHBDS mediates both the initial nucleation event (initial PPy deposition on the Al/Al_2O_3 surface) and the film growth stage (PPy deposition on PPy). Many more nucleation sites were observed in the presence of DHBDS than in control experiments where DHBDS was replaced by sodium *p*-toluenesulfonate (pTS).[19] Furthermore, the maximum potential reached in the presence of DHBDS during both the nucleation stage and the film growth stage was several hundred millivolts less positive than that observed in the control experiments (with pTS).[15]

Room temperature ionic liquids (RTILs) are increasingly being applied in electrochemistry[20] and have recently been explored as solvents for the electropolymerization of conducting polymers.[21–27] One of the earliest reports of electrodeposition of a CP from an ionic liquid described PPy deposition from a 1:l mol ratio of $AlC1_3$:*N*-1-butylpyridinium chloride molten salt at 40 °C,[21] a rather water sensitive ionic liquid. More recent work has employed air and water stable ionic liquids.[22–28] Generally, CPs prepared from ionic liquid solutions were found to be more electrochemically stable[22] and to possess smoother morphology and higher conductivity[27] than their counterparts formed from aqueous solution. These previous electrodepositions were all conducted on inert electrodes or on iron.[28] There have been no reports thus far on the direct electrodeposition of PPy on aluminum from ionic liquid solutions. We anticipate that electrodeposition of PPy on Al alloys from an ionic liquid might limit the oxide growth on the substrate (lack of a labile oxygen source, such as water) and would represent a green approach to electrodeposition (no volatile organic solvents used). Here, we describe the electrodeposition of PPy on aluminum alloy 2024-T3 from the ionic liquid 1-ethyl-3-methylimodazolium bis(trifluoromethanesulfonyl)imide, chosen because it has relatively high electronic conductivity and low viscosity[29] and readily dissolves the Py monomer.

Experimental

Chemicals

The 1-ethyl-3-methylimidazolium bis(trifluoromethanesulfonyl)imide ($EMIM^+TFSI^-$) was purchased from Covalent Inc. and was dried under reduced pressure overnight before use. Pyrrole was purchased from Aldrich Co. and was freshly distilled before use. AA 2024-T3 alloy panels were supplied by Q-panel (Cleveland, OH). The Al panels were polished by 600-grit SiC paper followed by degreasing with hexane. Ferrocene (Fc) was obtained from Aldrich Inc. and cobaltocenium hexafluorophosphate ($CcPF_6$) was obtained from VWR.

Determination of reference electrode potential

One challenge in performing electrochemistry in RTILs is establishing a known reference electrode potential. The approach used here was to calibrate a pseudo-reference electrode using well-characterized redox couples that were soluble in the ionic liquid. To that end, cyclic voltammetry was conducted in a three-electrode cell with a Ag wire pseudo-reference electrode (0.47 mm diameter), a platinum mesh working electrode and a platinum mesh counter electrode. Working electrode and auxiliary electrode were arranged parallel to each other in the $EMIM^+TFSI^-$ solution which contained 20 mM $CcPF_6$ and 5 mM Fc. The voltammetric scan originated –0.5 V and was swept positive to 0.8 V, negative to –1.3 V, then positive back to –0.5 V (vs the Ag wire pseudo-reference electrode) at a scan rate of 20 mV/s. All potentials reported below are with respect to the Ag wire electrode.

Electropolymerization of pyrrole

The electrochemical polymerization of Py was performed potentiodynamically in a one-compartment 20-mL three-electrode cell having an AA 2024-T3 working electrode (1 cm × 1 cm), a platinum mesh auxiliary electrode, and a silver wire pseudo-reference electrode. Some depositions were performed on indium tin oxide (ITO)-conducting glass electrodes. The working and auxiliary electrodes were arranged parallel to each other. The PPy films were deposited from 0.3 M Py in $EMIM^+TFSI^-$ solution. The potential was swept between 0 and 2.0 V for 20 cycles at a scan rate of 50 mV/s using an EG&G Princeton Applied Research potentiostat/galvanostat model 273A.

Characterization of polymers

Conductivity

Conductivity measurements were performed by the 4-point probe method (using a Signatone S-301 with tungsten carbide tips, a Keithley 220 current source, and a Keithley 2000 V) and also by conductive atomic force microscopy (C-AFM). C-AFM was performed using a Dimension 3100 scanner with a Nanoscope IIIa Controller and a Pt/Ir-coated cantilever (contact mode, 1–5 nN imaging force) employing a bias voltage of 50 mV. Topographical and current images were obtained simultaneously under ambient conditions and were collected in a scan range of 20 μm × 20 μm on 1 cm^2 PPy samples.

Scanning electron microscopy

Scanning electron microscopy (SEM) was applied to characterize the morphology and the thickness of the deposited film. The SEM data was collected using a JOEL JSM-6300 scanning electron microscope. A Technics Hummer II Sputter coater was used to coat all samples with a thin Au film. Energy dispersive X-ray spectroscopy information (EDX) was obtained via a ThermoNoran EDS detector using a Vantage Digital Acquisition Engine.

X-ray photoelectron spectroscopy

X-ray photoelectron spectroscopy (XPS) experiments were carried out with a Surface Science Instrument SSI-100 X-ray photoelectron spectrometer system equipped with an Al $K\alpha$ ($h\nu$ = 1486.6 eV) source under a base pressure of 2×10^{-9} torr. The percentages of elements were determined by normalized XPS peak area (C 1s peak for carbon, N 1s for nitrogen, F 1s for fluorine, O 1s for oxygen, S 2p for sulfur, and Al 2p for aluminum).

Cyclic Voltammetry

Cyclic voltammetry experiments were conducted in pure $EMIM^+TFSI^-$ ionic liquid employing a PPy covered ITO working electrode, a Pt mesh counter electrode, and a silver wire pseudo-reference electrode. The potential was swept at a scan rate of 20 mV/s.

Results and discussion

Reference electrode potential

There has been much discussion regarding reference electrodes for use in RTILs (reference 20, Ch. 3). The approach adopted here was that described previously,[30] whereby the potential of a Ag wire pseudo-reference electrode was calibrated with respect to the redox potential of ferrocenium (Fc^+)/ferrocene (Fc), since the redox potential of this couple is generally regarded as independent of solvent. Cyclic voltammetry was performed in $EMIM^+TFSI^-$ ionic liquid solution containing 5 mM Fc (and also, for comparison, 20 mM $CcPF_6$), with an example shown in Fig. 1. Based on five repetitions, the potential of silver wire pseudo-reference electrode was determined to be –0.110 (±0.005) V vs Fc^+/Fc and was quite stable from experiment to experiment. An additional advantage of the Ag wire pseudo-reference electrode was its small size, permitting placement very near the working electrode surface, thus minimizing ohmic polarization without significantly blocking current (hence, deposition of polymer) at the working electrode.

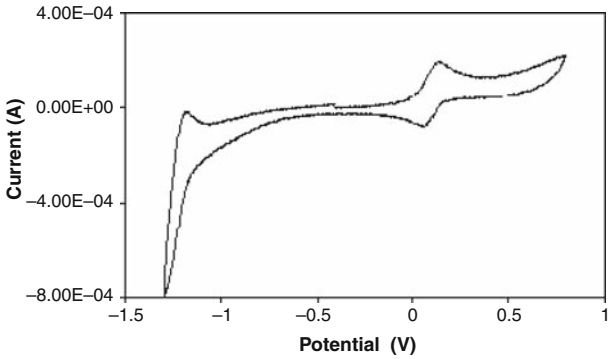

Fig. 1: Cyclic voltammogram of ferrocene (wave at 0.11 V) and cobaltocenium hexafluorophosphate (wave at –1.3 V) in $EMIM^+TFSI^-$ solution. The initial scan direction was positive, originating from –0.5 V vs Ag wire at a sweep rate of 20 mV/s

Electrochemical window

The electrochemical window of a RTIL is often quite large and indicates the potential range within which the ionic liquid is electrochemically inactive. Any impurities in the ionic liquid (e.g., water) will affect the electrochemical window. The linear scan voltammogram of Fig. 2 (curve 1) shows the electrochemical window for $EMIM^+TFSI^-$ at a Pt mesh electrode. Little or no current flows between –1.5 and 1.5 V, indicating little or no water present in the ionic liquid. The negative potential limit is due to the reduction of the $EMIM^+$ cation, whereas the positive potential limit is likely due to a combination of $EMIM^+$ and $TFSI^-$ oxidation.[20] RTILs based on the $EMIM^+$ cation have among the smallest potential windows.[20]

For comparison, an AA 2024-T3 electrode in the presence of Py yields a well-defined wave with an onset of ca. 1 V (Fig. 2, curve 2). Referenced to the standard hydrogen electrode scale (using $E°$ for

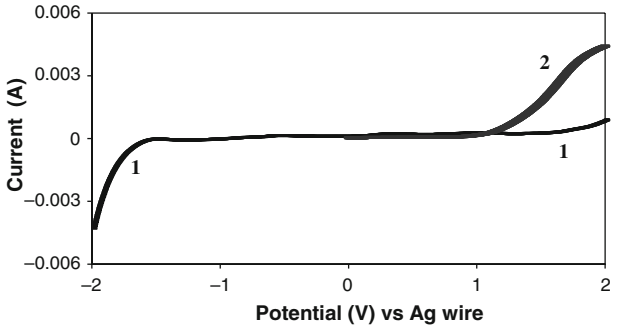

Fig. 2: *Curve 1*: Electrochemical window for $EMIM^+TFSI^-$ at a Pt mesh electrode. The potential sweep was from –2 V to 2 V vs. Ag wire at a scan rate of 20 mV/s. *Curve 2*: Linear sweep voltammogram of 0.3 M Py in $EMIM^+TFSI^-$ solution at a 1 cm^2 AA 2024-T3 electrode. Sweep was from 0 to 2 V at a scan rate of 20 mV/s

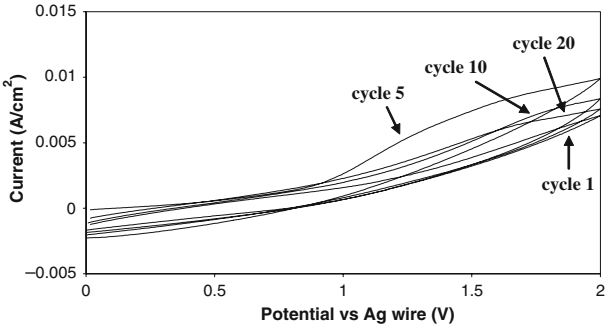

Fig. 3: Current–potential curves during the potentiodynamic electrodeposition of polypyrrole from 0.3 M pyrrole in $EMIM^+TFSI^-$ solution at 20 mV/s. Potential sweep initiated from 0 V

Fc of 0.47 V), the oxidation onset is ca. 1.56 V vs SHE. In aqueous solution without mediation, the oxidation onset is ca. 1.00 V vs SHE.[16] Much of this difference is attributed to ohmic polarization in the more resistive RTIL. Furthermore, the current density in the RTIL is significantly lower (ca. 7 mA/cm^2/M, measure 0.5 V beyond current onset) compared to that observed in the aqueous solution (ca. 50 mA/cm^2/M), reflecting the lower diffusion coefficient of Py in the more viscous RTIL. Diffusion coefficients in RTILs can be two to three orders of magnitude smaller than those in aqueous solution.[31] The wave in Fig. 2 was accompanied by the deposition of PPy as evidenced by visible polymer on the alloy surface at the end of the sweep.

Electrodeposition of PPy onto AA 2024-T3

The electrodeposition of PPy on AA 2024-T3 was carried out potentiodynamically. Attempts to deposit films galvanostatically (0.1 and 1 mA/cm^2) and potentiostatically (0.8, 1, and 1.5 V) were mostly unsuccessful, failing to provide uniform films on the aluminum substrate. Furthermore, electrodepositions attempted from three other ionic liquids (1-ethyl-3-methylimodazolium hexafluorophosphate, 1-ethyl-1-methylpyrrolidinium bis(trifluoromethanesulfonyl) imide, and 1-butyl-3-methylimodazolium hexafluorophosphate) yielded films that were less uniform than those generated from $EMIM^+TFSI^-$. This may be due to the lower viscosity and higher conductivity of $EMIM^+TFSI^-$.[29] The lower viscosity results in improved mass transport by diffusion, and the higher conductivity leads to reduced ohmic polarization (IR drop) and more uniform current density, resulting in more uniform polymer deposition. A slight discoloration of the $EMIM^+TFSI^-$ (from colorless to yellow) occurred during the deposition, probably reflecting small amounts of low molecular weight oligomers that dissolved in the RTIL. It has also been reported that the $TFSI^-$ anion leads to passivation of a magnesium alloy,[32] but a similar passivation of the aluminum alloy does not appear to occur in our experiments.

Figure 3 displays the current–potential curves observed during the potentiodynamic deposition. The current rapidly increased over the first five cycles as the polymer film formed, then slowly decreased as potential cycling continued. In electrodeposition from aqueous solutions at noble metal electrodes, the current typically increases with each cycle as the deposited film thickens. This behavior in $EMIM^+TFSI^-$ is likely due to the depletion of the Py monomer in the vicinity of the electrode surface (i.e., increasing concentration polarization) as a result of the slower diffusion of monomer in the rather viscous ionic liquid solution (compared to that in aqueous solution). Depositions under hydrodynamic conditions (i.e., with stirring) are planned.

Characterization of the deposited films

Film surface morphology and thickness

Optical microscopy and SEM were used to examine the surface morphology of the deposited films. The film surface was prepared for analysis by rinsing with acetone. The optical micrograph of Fig. 4 reveals that the Al alloy surface was completely covered by the PPy film. SEM images (Fig. 5) also confirm that the aluminum surface was completely covered by a compact PPy film. Elemental analysis by EDX (not shown) revealed no measurable Al, again indicating complete coverage of the surface. The thickness of the deposited PPy film was measured by SEM from cross-sectional images (Fig. 6). The film thickness varied over the range of 10–17 μm, a relatively thick and somewhat less uniform film compared to those prepared previously in our lab by electron transfer mediation.[15] Both the surface and cross-sectional SEM

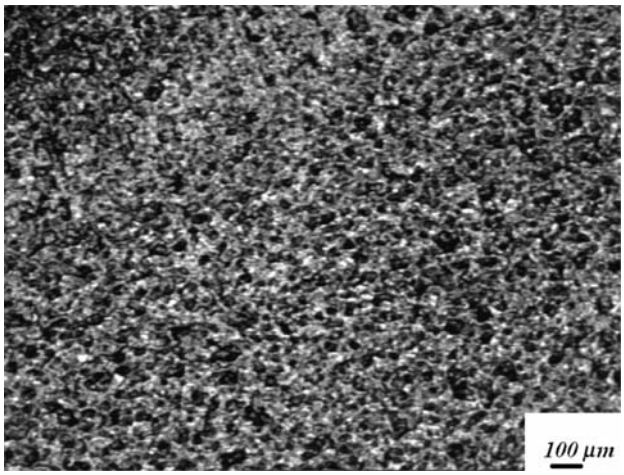

Fig. 4: Optical micrograph of the polypyrrole film

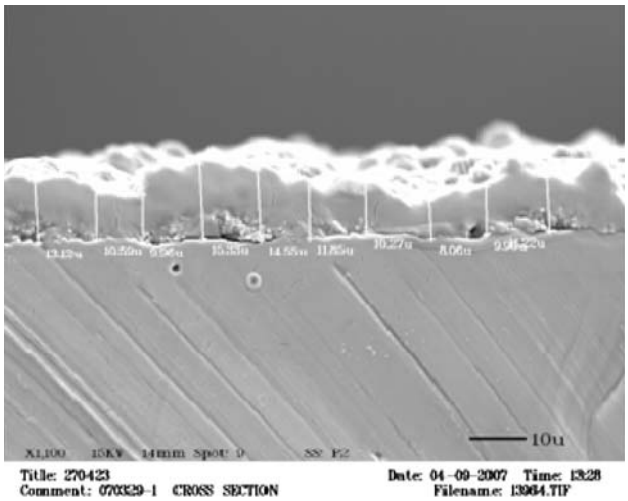

Fig. 6: SEM cross section of PPy/TFSI film (bar = 10 μm). Some indications of film thickness are displayed

images suggest a more compact or dense film than those prepared from aqueous solution using electron transfer mediation.[15]

Film analysis and doping level

EDX and XPS were used to determine the film composition. The EDX spectrum (not shown) revealed the presence of C, N, S, and O, the C/N arising from both the PPy backbone and the $TFSI^-$ anion incorporated into the polymer as the dopant anion and the S/O originating from only the anion. Figure 7 shows the XPS spectrum of the deposited film, confirming the EDX results and additionally exhibiting an intense F signal (ca. 687 eV). Thus, the anion of the RTIL was incorporated into the polymer as the dopant ion during electrodeposition. An estimate of the doping level can be obtained from the ratio of the atomic percentage of fluorine to that of nitrogen (ca. 2:1) obtained from the XPS spectrum. This ratio indicates a doping level of ca. 0.5, an average of one positive charge (thus, one

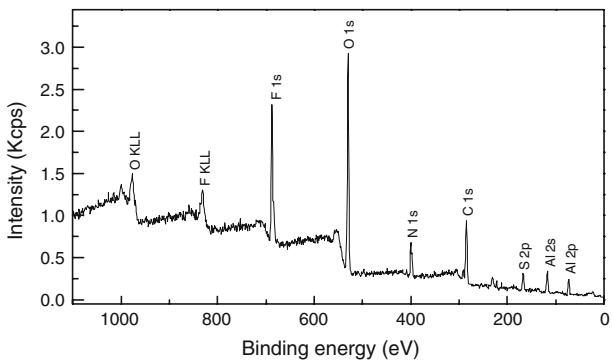

Fig. 7: XPS spectrum of the electrodeposited PPy/TFSI film

$TFSI^-$ anion) for every two monomer units in the polymer. This value is at the upper range of that normally observed for PPy and deserves further study.

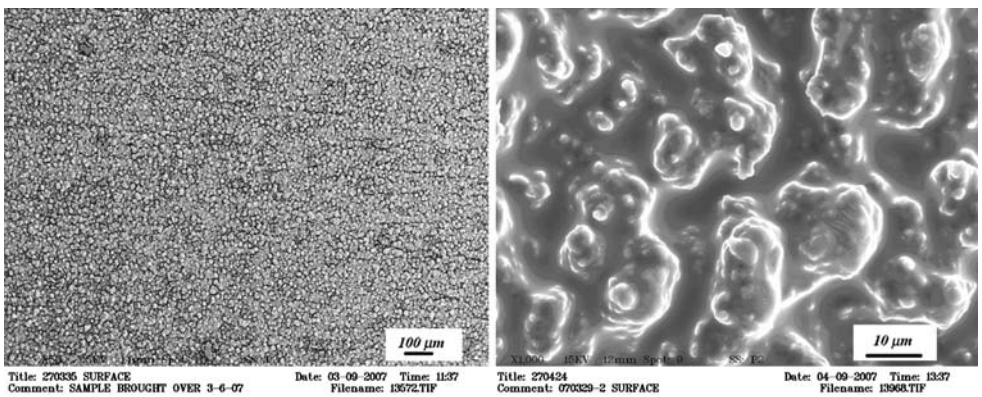

Fig. 5: SEM images of PPy/TFSI film (*left*: bar = 100 μm; *right*: bar = 10 μm)

Electroactivity of the deposited films

The electroactivity of the deposited films was assessed by cyclic voltammetry. Films deposited onto ITO and onto AA 2024-T3 were immersed in vacuum degassed $EMIM^+TFSI^-$ and the potential cycled from 0.3 V (OCP) to 1 to –1 V and back to 0.3 V at 100 mV/s. The results, shown in Fig. 8, reveal that the films deposited on both ITO and on AA 2024-T3 are indeed electroactive and maintain their activity from cycle to cycle. For comparison, a background CV at the bare alloy (no PPy film) reveals little or no current over the same range of potential. The voltammograms are clearly distorted due to ohmic polarization arising from the RTIL resistance.

Conductivity of the PPy/TFSI film

The conductivity of the electrodeposited film was measured using two methods, the 4-point probe method and C-AFM. The 4-point probe measures film surface conductivity and yielded an average value of 0.15 ± 0.06 S/m with very poor reproducibility. This is a rather low conductivity compared to that of films we have deposited from aqueous solution (typically >10 S/m).[15]

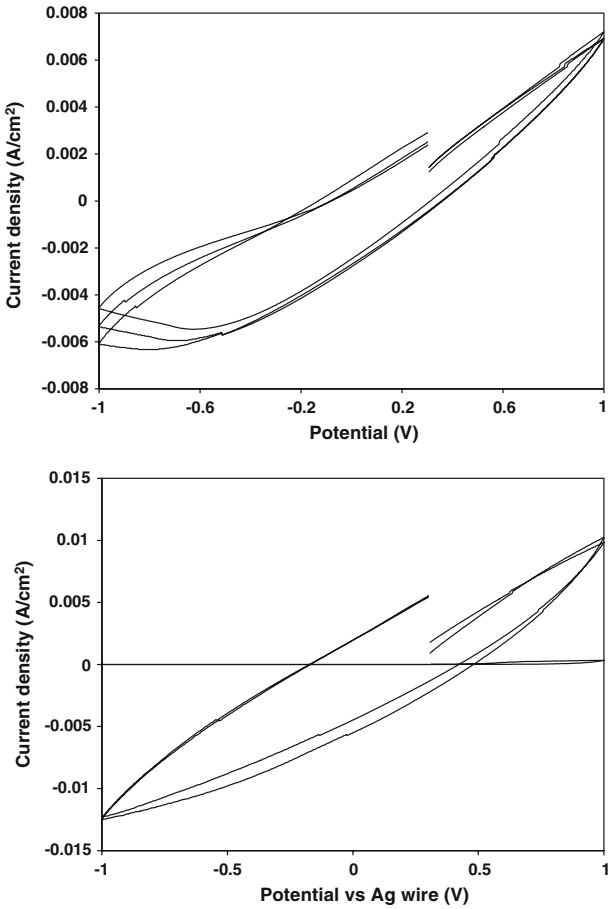

Fig. 8: Cyclic voltammograms of $PPy/TFSI^-$ films in $EMIM^+TFSI^-$ originating from 0.3 V and sweeping to 1 V to –1 V, then back to 0.3 V at 100 mV/s. *Top*: $PPy/TFSI^-$ on ITO showing cycles 1, 2, and 5 (top to bottom). *Bottom*: $PPy/TFSI^-$ on AA 2024-T3 showing cycles 1 (*top*) and 5 (*bottom*). Also shown is the background voltammogram of freshly polished bare alloy in the ionic liquid (horizontal curve at zero current)

Conductive AFM provides a measure of the local conductivity through the film from the AFM tip to the underlying substrate. In some ways we consider this a more reliable method of assessing and comparing thin film conductivity since very little force (1–5 nN) is exerted on the AFM cantilever compared to that exerted by the manual 4-point probe method which subjects the film to possible damage. C-AFM typically gives a much higher value of conductivity, often by a factor of 100 or more, than does the 4-point probe. Some of this difference may reflect anisotropy in film conductivity, since the C-AFM current path is predominately in the direction of the film thickness, whereas the 4-point probe current path is predominately horizontal to the film surface. Figure 9 shows the contact mode surface topography and current images for the PPy/TFSI film. The topography image is consistent with the SEM image of Fig. 5 and shows a somewhat rougher surface than that obtained by mediated electrodeposition from aqueous solution.[18] Interestingly, the conductivity image reveals a rather uniform conductivity across the surface, the current averaging ca. 0.5 nA across the surface for a 50 mV bias potential. From the film thickness and the estimated tip contact area (19.5 nm^2), an average conductivity of 7700 S/m is computed from three samples. This value falls within the range of 5000 to 20,000 S/m measured by C-AFM for PPy films deposited on AA 2024-T3 from aqueous solution.[33]

Adhesion

Quantitative measurement of adhesion was not made due to the small substrate area (1 cm^2) used in these experiments (to conserve the volume of RTIL required). A simple tape pull-off test revealed no polymer removal, but scribing the film with a scalpel resulted in detachment of some polymer. Thus, the adhesion is modest, but does not appear to be as high as that obtained by mediated electrodeposition from aqueous solution.[15]

Conclusions

The electrodeposition of PPy films from ionic liquid solutions at AA 2024-T3 was successfully carried out by using the RTIL 1-ethyl-3-methylimidazolium bis(trifluoromethanesulfonyl)imide. Potentiodynamic deposition gave the best results, producing films that completely covered the alloy surface. The films appeared to be more dense and less uniform than

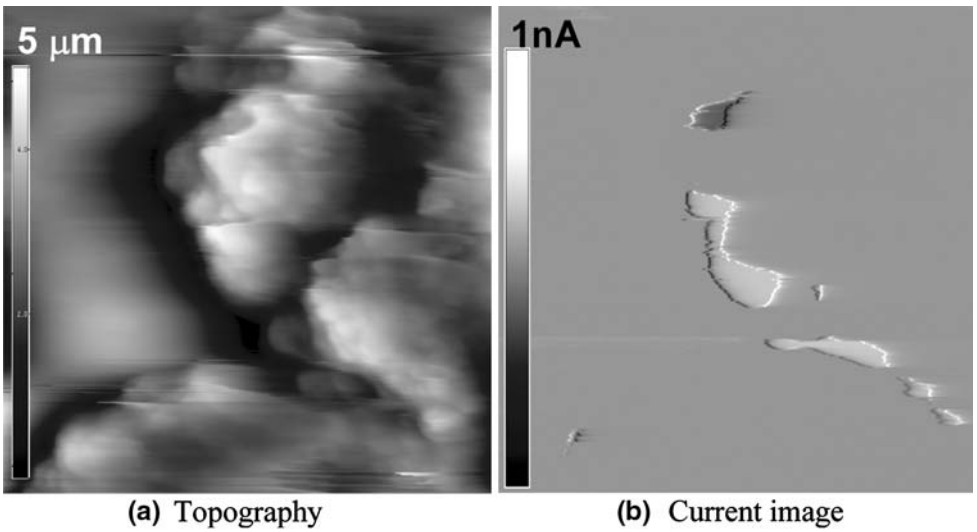

Fig. 9: Contact mode AFM (*left*) and C-AFM (*right*) images of PPy/TFSI film. Each image is 5 μm × 5 μm in area

those deposited by mediated electrodeposition from aqueous solution, but no evidence of interference due to oxide growth on the Al alloy was observed. The PPy films were doped by the $TFSI^-$ anion of the RTIL and exhibited electronic conductivity as well as stable electroactivity. RTILs provide a useful solvent/electrolyte medium for electrodepositing CPs onto active metals and further work in under way.

Acknowledgments This work was supported by the Air Force Office of Scientific Research (grant no. FA9550-06-1-0461). The authors would also like to thank Dr. Hosup Jung (C-AFM), Dr. Jinhai Wang (XPS), and Mr. Scott Payne (SEM) for their assistance in the characterization of the films.

References

1. Battocchi, D, Simões, AM, Tallman, DE, Bierwagen, GP, ''Electrochemical Behaviour of a Mg-Rich Primer in The Protection of Al Alloys.'' *Corros. Sci*, **48** 1292–1306 (2006)
2. Tallman, DE, Pae, Y, Bierwagen, GP, ''Conducting Polymers and Corrosion: Part 2—Polyaniline on Aluminum Alloys.'' *Corrosion*, **56** 401–410 (2000)
3. He, J, Gelling, VJ, Tallman, DE, Bierwagen, GP, Wallace, GG, ''Conducting Polymers and Corrosion III. A Scanning Vibrating Electrode Study of Poly(3-octyl pyrrole) on Steel and Aluminum.'' *J. Electrochem. Soc.*, **147** 3667–3672 (2000)
4. Gelling, VJ, Wiest, MM, Tallman, DE, Bierwagen, GP, Wallace, GG, ''Electroactive-Conducting Polymers for Corrosion Control 4. Studies of Poly(3-octyl pyrrole) and Poly(3-octadecyl pyrrole) on Aluminum 2024-T3 Alloy.'' *Prog. Org. Coat.*, **43** 149–157 (2001)
5. Tallman, DE, Spinks, GM, Dominis, AJ, Wallace, GG, ''Electroactive Conducting Polymers for Corrosion Control Part 1. General Introduction and a Review of Nonferrous Metals.'' *J. Solid State Electrochem.*, **6** 73–84 (2002)
6. Tallman, DE, He, J, Gelling, VJ, Bierwagen, GP, Wallace, GG, ''Scanning Vibrating Electrode Studies of Electroactive Conducting Polymers on Active Metals.'' In: Zarras, P, Stenger-Smith, JD, Wei, Y (eds.) *Electroactive Polymers for Corrosion Control*, ACS Symposium Series 843, Washington, DC (2003)
7. He, J, Tallman, DE, Bierwagen, GP, ''Conjugated Polymers for Corrosion Control: Scanning Vibrating Electrode Studies of Polypyrrole-Aluminum Alloy Interactions.'' *J. Electrochem. Soc.*, **151** B644–B651 (2004)
8. Spinks, GM, Dominis, AJ, Wallace, GG, Tallman, DE, ''Electroactive Conducting Polymers for Corrosion Control Part 2. Ferrous Metals.'' *J. Solid State Electrochem.*, **6** 85–100 (2002)
9. Tallman, DE, Bierwagen, GP, ''Corrosion Protection Using Conducting Polymers,'' *Chapter 15 in Handbook of Conducting Polymers*, *Conjugated Polymers-Processing and Applications*, 3rd ed, pp. 15–1 to 15–53. CRC Press, Florida (2007)
10. Beck, F, Huelser, P, ''Electrodeposition of Polypyrrole on Aluminum from Nonaqueous Solutions.'' *J. Electroanal. Chem.*, **280** 159–166 (1990)
11. Huelser, P, Beck, F, ''Electrodeposition of Polypyrrole Layers on Aluminum from Aqueous Electrolytes.'' *J. Appl. Electrochem.*, **20** 596–605 (1990)
12. Naoi, K, Takeyuki, M, Kanno, H, Sakakura, M, Shimada, A, ''Simultaneous Electrochemical Formation of Al_2O_3/Polypyrrole Layers (I): Effect of Electrolyte Anion in Formation Process.'' *Electrochim. Acta*, **45** 3413–3421 (2000)
13. Hien, NTL, Garcia, B, Pailleret, A, Deslouis, C, ''Role of Doping Ions in The Corrosion Protection of Iron by Polypyrrole Films.'' *Electrochim. Acta*, **50** 1747–1755 (2005)
14. Saidman, SB, Vela, ME, ''Electropolymerization of Pyrrole Onto Aluminium from Alkaline Solutions Containing a Surfactant.'' *Thin Solid Films*, **493** 96–103 (2005)
15. Tallman, DE, Vang, C, Wallace, GG, Bierwagen, GP, ''Direct Electrodeposition of Polypyrrole on Aluminum and Aluminum Alloy by Electron Transfer Mediation.'' *J. Electrochem. Soc.*, **149** C173–C179 (2002)
16. Tallman, DE, Vang, CK, Dewald, MP, Wallace, GG, Bierwagen, GP, ''Electron Transfer Mediated Deposition of Conducting Polymers on Active Metals.'' *Synth. Met.*, **33** 135–136 (2003)

17. Tallman, DE, Dewald, MP, Vang, CK, Wallace, GG, Bierwagen, GP, ''Electrodeposition of Conducting Polymers on Active Metals by Electron Transfer Mediation.'' *Curr. Appl. Phys.*, **4** 137–140 (2004)
18. Levine, KL, Tallman, DE, Bierwagen, GP, ''The Mediated Electrodeposition of Polypyrrole on Aluminium Alloy.'' *Aust. J. Chem.*, **58** 294–301 (2005)
19. Yang, XF, Tallman, DE, Croll, SG, Bierwagen, GP, ''Electrodeposition of Polypyrrole on Aluminum Alloy.'' *Proceedings of the International Conference on Surface Modification Technologies*, Indianapolis, IN, 2001
20. Ohno, H, *Electrochemical Aspects of Ionic Liquids*. Hoboken, New Jersey (2005)
21. Pickup, PG, Osteryoung, RA, ''Electrochemical Polymerization of Pyrrole and Electrochemistry of Polypyrrole Films in Ambient Temperature Molten Salts.'' *J. Am. Chem. Soc.*, **106** 2294–2299 (1984)
22. Lu, W, Fadeev, AG, Qi, B, Smela, E, Mattes, BR, Ding, J, Spinks, GM, Mazurkiewicz, J, Zhou, D, Wallace, GG, MacFarlane, DR, Forsyth, SA, Forsyth, M, ''Use of Ionic Liquids for π-Conjugated Polymer Electrochemical Devices.'' *Science*, **297** 983–987 (2002)
23. Sekiguchi, K, Atobe, M, Fuchigami, T, ''Electropolymerization of Pyrrole in 1-ethyl-3-methylimidazolium Trifluoromethanesulfonate Room Temperature Ionic Liquid.'' *Electrochem. Commun.*, **4** 881–885 (2002)
24. Boxall, DL, Osteryoung, RA, ''Switching Potentials and Conductivity of Polypyrrole Films Prepared in the Ionic Liquid 1-Butyl-3-methylimidazolium Hexafluorophosphate.'' *J. Electrochem. Soc.*, **151** E41–E45 (2004)
25. Zhang, J, Zhang, X, Fang, X, Hu, F, ''Effect of Polar Solvent Acetonitrile on The Electrochemical Behavior of Polyaniline in Ionic Liquid Electrolytes.'' *J. Colloid Interf. Sci.*, **287** 67–71 (2005)
26. Pringle, JM, Efthimidadis, J, Howlett, PC, Efthimiadis, J, MacFarlane, DR, Chaplin, AB, Hall, SB, Officer, DL, Wallace, GG, Forsyth, M, ''Electrochemical Synthesis of Polypyrrole in Ionic Liquids.'' *Polymer*, **45** 1447–1453 (2004)
27. Li, M, Ma, C, Liu, B, Jin, Z, ''A Novel Electrolyte 1-ethylimidazolium trifluoroacetate Used for Electropolymerization of Aniline.'' *Electrochem. Commun.*, **7** 209–212 (2005)
28. Fenelon, AM, Breslin, CB, ''The Formation of Polypyrrole at Iron from 1-Butyl-3-Methylimidazolium Hexafluorophosphate.'' *J. Electrochem. Soc.*, **152** D6–D11 (2005)
29. Bonhote, P, Dias, A, Papageorgiou, N, Papageorgiou, N, Kalyanasundaram, K, Graetzel, M, ''Hydrophobic, Highly Conductive Ambient-Temperature Molten Salts.'' *Inorg. Chem.*, **35** 1168–1178 (1996)
30. Snook, GA, Best, AS, Pandolfo, AG, Hollenkamp, AF, ''Evaluation of a Ag|Ag+ Reference Electrode for Use in Room Temperature Ionic Liquids.'' *Electrochem. Commun.*, **8** 1405–1411 (2006)
31. Zhang, J, Bond, AM, ''Practical Considerations Associated with Voltammetric Studies in Room Temperature Ionic Liquids.'' *Analyst*, **130** 1132–1147 (2005)
32. Forsyth, M, Howlett, PC, Tan, SK, MacFarlane, DR, Birbilis, N, ''An Ionic Liquid Surface Treatment for Corrosion Protection of Magnesium Alloy AZ31.'' *Electrochem. Solid-State Lett.*, **9** B52–B55 (2006)
33. Jung H, Tallman DE, ''Morphological and Electrical Characterization of Polypyrrole-Polystyrenesulfonate films on AA 2024-T3 Alloy.'' North Dakota State University (unpublished results) (2007)